

uid crystal surrounding the isotropic droplet can be changed applying an electric field surrounding the device with conducting (ITO-coated) glasses (Fig. 1). The polarization state of the light impinging on the rear polarizer is a function of the applied field and therefore the nonlinear behavior of the device can be controlled by the external electric field.

We have studied two devices—the first (*P* device) is constructed with parallel polarizers; the second (*C* device) with crossed polarizers—and developed a simple model to describe their behavior.

The *P* device shows self-transparency effect, while the *C* device shows optical bistability.

Experimental measures of the transmittance of both the *P* and *C* devices are shown. The experimental data are compared with predictions based on our model.

*INFM-Dip. Scienze Fisiche

**INFM Unità di Napoli

1. L. Vicari, F. Bloisi, F. Simoni, Opt. Commun. 80, 338–392 (1991).
2. L. Vicari, F. Bloisi, F. Simoni, Appl. Phys. B 53, 314–318 (1991).

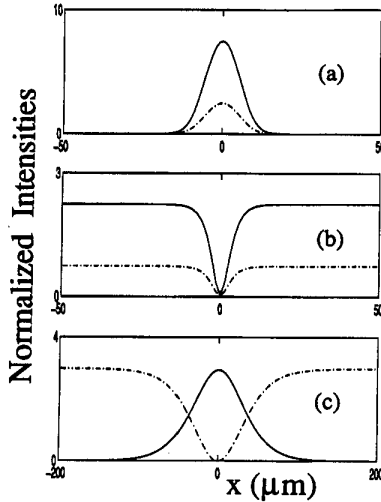
QWE22

Incoherently coupled soliton pairs in biased photorefractive crystals

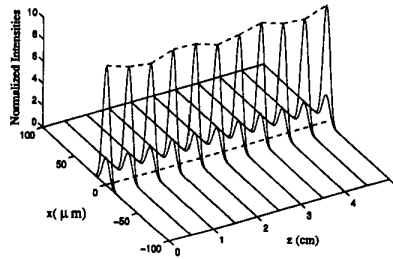
S. R. Singh, D. N. Christodoulides, M. I. Carvalho, M. Segev,* Department of Electrical Engineering and Computer Science, Lehigh University, Bethlehem, Pennsylvania 18015

Recently it was demonstrated that spatial optical solitons at μW power levels can be supported in photorefractive (PR) media.^{1–6} In particular, the so-called screening solitons are possible when an external bias voltage is appropriately applied to a PR crystal.^{2,3} Moreover, the optical beam is required to be linearly polarized. Very recently, vector solitons involving the two polarization components have also been predicted in biased PR materials.^{7,8} This latter class of solitons can only be achieved in specific system geometries.

We show that a new type of incoherently coupled soliton pairs is possible under steady-state conditions provided that their carrier beams share the same polarization and wavelength and are mutually incoherent. They can be readily realized in a simple experimental setup where the optical beams co-propagate collinearly in a biased PR crystal, in which case they experience equal electro-optic coefficients. The two optical beams can be also slightly misaligned at the input so as to differentiate them at the output plane.^{9,10} To start, let us consider two one-dimensional optical beams that are polarized parallel to the *c* axis (*x* axis) in a strontium niobate (SBN) PR crystal. Moreover, under strong bias conditions and for relatively broad beam configurations, the steady-state space charge electric field is approximately given by^{2,3}



QWE22 Fig. 1 Soliton components, $|U|^2$ (solid curve) and $|V|^2$ (dash-dot curve), for a (a) bright-bright pair when $r = 10$ and $\theta = 30^\circ$, (b) dark-dark pair when $\rho = 3$ and $\theta = 30^\circ$, and (c) bright-dark pair when $\rho = 3$ and $\delta = -0.01$.



QWE22 Fig. 2 Stable propagation of a ($r = 10$, $\theta = 30^\circ$) bright-bright soliton pair when its larger intensity component is perturbed by 20% at the input.

$$E_s(x, z) = E_0 \frac{(I_d + I_s)}{I_d + I(x, z)} \quad (1)$$

where $I(x, z)$ is total power density of the two optical beams, I_d is the so-called dark irradiance, and I_s represents the total power density soliton pair attains away from the center of the PR crystal. E_0 is value of the electric field at $x \rightarrow \pm\infty$ and is approximately V_{ext}/W , where V_{ext} is the external bias applied along the *x*-width *W* of the crystal. In such a case, it can be readily shown that normalized beam envelopes U, V , where $U = (n_e/2\eta_0 I_d)^{1/2} \phi$ and $V = (n_e/2\eta_0 I_d)^{1/2} \psi$, $[I = (n_e/2\eta_0)(|\phi|^2 + |\psi|^2)]$, obey the following paraxial evolution equations:

$$iU_\xi + \frac{U_{xx}}{2} - \beta(1 + \rho) \frac{U}{1 + |U|^2 + |V|^2} = 0 \quad (2)$$

$$iV_\xi + \frac{V_{xx}}{2} - \beta(1 + \rho) \frac{V}{1 + |U|^2 + |V|^2} = 0, \quad (3)$$

where $U_\xi = \partial U / \partial \xi$ etc. and $\rho = I_s / I_d$ and $\beta = (k_0 x_0)^2 n_e^4 r_{33} E_0 / 2$. $k_0 = 2\pi / \lambda_0$, n_e is the extraordinary index of refraction and r_{33} is the electro-optic coefficient involved. Moreover, in Eqs. (2) and (3) the following simplifying transformations have been used: $\xi = (z/k_0 n_e x_0^2)$ and $s = x/x_0$, where x_0 is an arbitrary scaling parameter.

Let us now solve Eqs. (2) and (3) by first considering a bright-bright soliton pair. To do so, the envelopes U and V are expressed in the following fashion: $U = r^{1/2} y(s) \cos \theta \exp(i\mu\xi)$ and $V = r^{1/2} y(s) \sin \theta \exp(i\mu\xi)$. μ represents a nonlinear shift of the propagation constant, $y(s)$ is a normalized real function bounded between $0 \leq y(s) \leq 1$, and the parameter θ is an arbitrary projection angle. In turn, it can be readily shown that $y(s)$ obeys the singly polarized bright soliton equation. In this case, the soliton pair components can be considered as the θ projections of the fundamental bright soliton envelope. Figure 1a shows a normalized intensity profile of the soliton pair obtained at $r = 10$ and $\theta = 30^\circ$ for typical SBN crystal parameters. Also shown in Fig. 1 is a dark-dark soliton profile that can be obtained (Fig. 1b) in a similar fashion.

Finally, bright-dark soliton pairs are also possible. To obtain them, the envelopes U and V are expressed in the following way: $U = r^{1/2} f \exp(i\mu\xi)$ and $V = \rho^{1/2} g \exp(i\mu\xi)$, where f corresponds to a bright beam envelope and g to a dark one. An approximate solution set can then be obtained provided that $f^2 + g^2 = 1$, and it is given by

$$U = r^{1/2} \text{sech}[(\beta\delta)^{1/2}s] \cdot \exp[-i\beta(1 - \delta/2)\xi] \quad (4)$$

$$V = \rho^{1/2} \tanh[(\beta\delta)^{1/2}s] \exp[i\beta\xi]. \quad (5)$$

An example of the above pair is shown in Fig. 1c.

The stability properties of the soliton pairs were also investigated with use of numerical methods. The bright-bright and dark-dark pairs were found to be stable against small perturbations. Figure 2 depicts the evolution of the pair component when the high intensity beam has been perturbed by 20%. Bright-dark pairs were found to be stable only in the regime where the applied bias (or β) is negative.

*Department of Electrical Engineering and Advanced Center for Photonics and Optoelectronic Materials and Princeton Material Institute, Princeton University, Princeton, New Jersey 08544

1. M. Segev, B. Crosignani, A. Yariv, B. Fischer, Phys. Rev. Lett. 68, 923 (1992).
2. M. Segev, G. C. Valley, B. Crosignani, P. DiPorto, A. Yariv, Phys. Rev. Lett. 73, 3211 (1994).
3. D. N. Christodoulides, M. I. Carvalho, J. Opt. Soc. Am. B 12, 1628 (1995).
4. G. Duree, G. Salamo, M. Segev, A. Yariv, B. Crosignani, P. D. Porto, E. Sharp, Opt. Lett. 19, 1195 (1994).
5. M. D. Castillo, P. A. Aguilar, J. J. Mondragon, S. Stepanov, V.

- Vysloukh, *Appl. Phys. Lett.* **64**, 408 (1994).
6. M. Shih, M. Segev, G. C. Valley, G. Salamo, B. Crosignani, P. DiPorto, *Electron. Lett.* **31**, 826 (1995).
 7. M. Segev, G. C. Valley, S. R. Singh, M. I. Carvalho, D. N. Christodoulides, *Opt. Lett.* **20**, 1764 (1995).
 8. M. I. Carvalho, S. R. Singh, D. N. Christodoulides, R. I. Joseph, to appear in *Phys. Rev. E*.
 9. M. D. I. Castillo, J. J. Sanchez-Mondragon, S. I. Stepanov, M. B. Klein, B. A. Wechsler, *Opt. Comm.* **118**, 515 (1995).
 10. P. A. M. Aguilar, J. J. Sanchez-Mondragon, S. Stepanov, G. Bloch, *Opt. Comm.* **118**, 165 (1995).

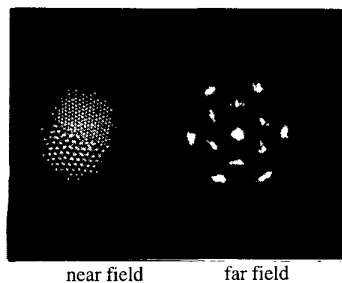
QWE23

Multiple scale hexagonal patterns

A. V. Mamaev, M. Saffman,* *Institute for Problems in Mechanics, Russian Academy of Sciences, Prospekt Vernadskogo 101, Moscow, 117526 Russia*

Hexagonal optical patterns appear as a result of a transverse instability of counterpropagating laser beams in a nonlinear medium. In large aspect ratio experiments, where transverse boundary conditions play only a weak role, a single spatial scale characterizes the hexagons. This scale results from a compatibility condition between different mechanisms. In transverse nonlinear optics a resonance occurs when a nonlinear phase shift resulting from, e.g., a cubic nonlinearity, cancels the linear diffractive phase shift because of propagation. The resulting transverse patterns have a characteristic spatial scale given by $\sqrt{\lambda l}$, where λ is the optical wavelength and l is the length of the nonlinear medium.

When the nonlinear medium is placed in an optical cavity that provides feedback, additional resonances come into play. By use of the polished end faces of the nonlinear medium, here a 5-mm-long photorefractive crystal of KNbO₃, as a weakly reflecting Fabry-Perot cavity new spatial scales corresponding to cavity resonances are selected. An example, showing simultaneous excitation of two distinct scales, is shown in Fig. 1. We present a range of experimental data showing excitation of a single scale, with



QWE23 Fig. 1 Experimental observation of a multiple scale hexagonal pattern.

the scale fixed by the cavity tuning, excitation of multiple scales, and excitation of multiple hexagons exhibiting near-field grain boundaries at a single scale. We have studied the coexistence of multiple scales theoretically on the basis of a dispersion relation that accounts for the influence of the cavity resonances.

**Department of Optics and Fluid Dynamics, Risø National Laboratory, Postbox 49, DK-4000 Roskilde, Denmark*

QWE24

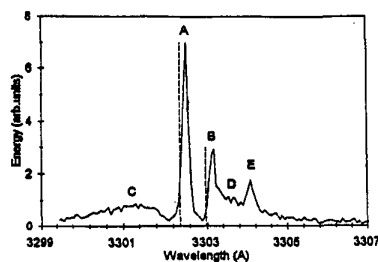
Tunable, up-converted stimulated ultraviolet Mollow triplet via four-wave mixing

L. Moorman, I. Pop, *Department of Physics and Astronomy, University of Wyoming, PO Box 3905, Laramie, Wyoming 82071*

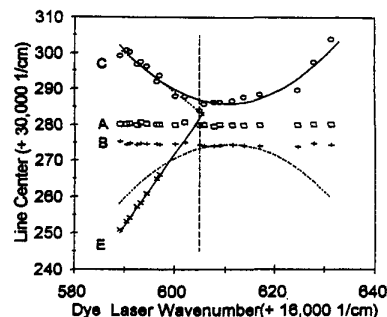
Two new types of upward-converted, tunable, stimulated ultraviolet emissions and one fixed frequency type are generated via two-photon near-resonant $3S_{1/2}$ - $5S_{1/2}$ pumping of a Na vapor.¹ All observed tunable components near 330 nm are associated with the $J = 3/2$ multiplet and none with the $J = 1/2$ multiplets of $4P$ state.

A fixed frequency ultraviolet emission (Type 0) is generated in a two-step process in which infrared tunable hyper-Raman radiation is generated that is utilized in a four-wave mixing process with two laser photons to generate a fixed frequency ultraviolet emission that is red-shifted compared with the atomic transition, shown as peaks A and B in Fig. 1. The two lines associated with the $4P_{3/2}$ and $4P_{1/2}$ multiplets show inversion of relative line strength close to the two-photon pump resonance, compared with a statistical model and normal line strength at larger detunings.

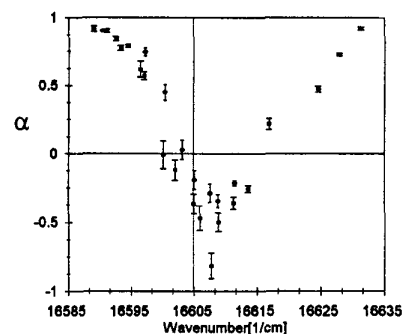
Type I tunable ultraviolet stimulated emission is generated in a two-step process involving four-wave mixing of an ASE, infrared photon, resulting in linear ultraviolet tunability (E in Figs. 1 and 2). Type II tunable stimulated emission employs three steps: infrared hyper-Raman scattering, four-wave mixing, and ac-Stark splitting. Type 2 is induced by Type 0 ultraviolet radiation strong enough to



QWE24 Fig. 1 Typical ultraviolet spectrum with negative detuned two-photon ($3S$ - $5S$) linearly polarized focused pump. Dashed vertical curves indicate the $4P$ - $3S$ resonances for $j = 3/2$ and $j = 1/2$ multiplets.



QWE24 Fig. 2 Ultraviolet shifts as a function of two-photon pump detuning.



QWE24 Fig. 3 Asymmetry of the two side components of the stimulated Mollow triplet as a function of pump detuning.

create ac-Stark splitting described by the dressed atom model for the $3S_{1/2}$ and $4P_{3/2}$ states. As a consequence Type II produces two side components (C, D) besides the central component (A) that together can be interpreted as a stimulated ultraviolet Mollow triplet. The side components (C, D) are broadened by the different ultraviolet intensities over the cross section of the beam at the focus. The Rabi frequency measured from a quadratic fit to the measured shifts of peak D with the two-photon pump detuning shown in Fig. 2 determines the value of the generated UV intensity at the focus. The value is consistent with a direct measurement of the integrated pulse energy. The model also explains measured spatial beam cross section patterns.

A study of observed asymmetries between the two side components of the stimulated Mollow triplet is currently investigated.² Preliminary data shown in Fig. 3, with α a measure of the asymmetry $[(C - D)/(C + D)]$, show that near the resonance the red-shifted component is dominant whereas far off resonance the blue-shifted component has the larger line strength. By reflecting the forward-generated light back through the vapor, we measured a systematic increase of relative strength of the blue side component in the backward spectra compared with the forward spectra. A qualitative explanation can be given at this time; a full